

PERFORMANCE EVALUATION OF BUILDING FAÇADE RECONSTRUCTION FROM UAS IMAGERY

Edward R. Clay¹, Kara S. Lee¹, Sheng Tan¹, Long Ngo Hoang Truong², Omar E. Mora^{1*}, Wen Cheng¹

¹Civil Engineering Department, California State Polytechnic University, Pomona, USA – (erclay, karalee, shengtan, oemora, and wcheng)@cpp.edu

²Department of Computer Science, California State Polytechnic University, Pomona, USA – ltruong@cpp.edu

KEY WORDS: Unmanned Aircraft System (UAS), Ground Control Point (GCP), Photogrammetry, Point Cloud, Cloud-to-Cloud (C2C), Accuracy, Reconstruction.

ABSTRACT:

Unmanned Aircraft Systems (UASs) coupled with low-cost cameras are rapidly becoming a cost-effective alternative for surveying and mapping, particularly for civil, construction, and environmental engineering applications. The proliferation of UASs provide unique opportunities to map and model surfaces at unprecedented spatial and temporal resolutions. Although, UASs have been extensively evaluated for mapping and modeling, limited research has been performed on assessing the accuracy of UAS imagery for building façade reconstruction. In this study, a performance evaluation of UAS mapping for building façade reconstruction is performed. Our results suggest that there are many aspects that impact the accuracy of UAS photogrammetry for building façade reconstruction. In specific, the texture, contrast, and subtle details influence the generated point cloud, thus complicating the building façade reconstruction. The best results were obtained by strategizing the flying height and camera angle; where, the mean, median, and standard deviation for the cloud-to-cloud (C2C) absolute distances were 0.023, 0.014, and 0.023 meters, respectively, by applying a flying height of 150' with an orbit at 80'. Therefore, it may be concluded that UAS photogrammetric mapping can meet sub-decimeter accuracy for building façade reconstruction, if proper planning, data collection and processing procedures are followed.

1. INTRODUCTION

Photogrammetry is the process in which information is obtained regarding objects' properties without the need for physical contact (Mikhail, 2001). Current photogrammetric methods are usually divided into two distinct groups: terrestrial photogrammetry (Aber et al., 2010). While this method is useful in gathering information at a distance, terrestrial photogrammetry still requires someone to be on-site, potentially exposed to any hazards present on-site, and potentially having to deal with unstable ground that could also affect image quality (Erlandson and Veress, 1974). The more recent type of photogrammetry is aerial photogrammetry.

As the name suggests, aerial photogrammetry is taking images from an aerial point of view. Originally, this included taking photographs from airplanes which allow for larger expanses of land to be recorded in short amounts of time; however, this method has been flawed due to the need for adequate elevation, preventing the ability to obtain more detailed photos of specific structures (Sowmya and Trinder, 2000). In more recent years, aerial photogrammetry has become more popular due to the improvements and availability in Unmanned Aircraft Systems (UASs). UAS, paired with different vision-based systems and computer vision algorithms, provide opportunities to collect, process, and reconstruct the three-dimensional (3D) position of surface features (Colomina and Molina, 2014). UASs combined with these vision-based systems provide distinct advantages for noncontact, high temporal, and spatial resolution data (Rakha and Gorodetsky, 2018; Mora et al., 2019). For these reasons, UASs have been utilized in determining the elevation of road runoff (Díaz-Vilaríño et al., 2016), glaciological measurements (Whitehead et al., 2013), as well as georeferencing (Gabrlík, 2015), to name a few applications.

Since the mid-2000s, there has been a significant step towards utilizing photogeometric methods to measure critical features on buildings (Shashi and Jain, 2007; Grussenmeyer et al., 2008; Galantucci and Fatiguso, 2019). Much due to the advancements in UASs, these systems have also seen use in mapping key

features in buildings (Ajayi, 2018). This is primarily due to the availability and ease of use that UASs systems have and improvements in the methodology to refine image quality (Eschmann et al., 2012; Adams et al., 2014). Despite the promising results that previous studies have shown, there is still an apparent lack of studies that assess the performance of these systems (Peppas et al., 2019). A similar lack of studies has also focused on UASs systems using cloud-to-cloud (C2C) point accuracy to assess these systems (Martinez et al., 2021). For these reasons, it is crucial to perform an accuracy assessment of UAS collected data using C2C point accuracy.

In this study, a building was reconstructed using a UAS. Three independent flights were performed involving a different flying height and camera angle. To evaluate the performance of building façade reconstruction from UAS imagery the building was scanned using a Terrestrial Laser Scanner (TLS). Subsequently, the UAS imagery and TLS data was processed for comparison. The best results of the mean, median, and standard deviation of the C2C were 0.023, 0.014, and 0.023 meters, respectively, with a flying height of 150' and an orbit of 80'. Therefore, it may be concluded that the use of UAS photogrammetric mapping for building façade reconstruction can meet sub-decimeter accuracy as long as proper planning, data collection, and processing procedures are followed.

2. MATERIALS AND METHODS

The procedure used to evaluate the photogrammetric mapping accuracy of building façade reconstruction from UAS imagery is summarized in Figure 1.

2.1 Study Area

The study area is a rectangular building located in Ontario, California, United States of America (Latitude: 34° 04' 22.90" N, Longitude: 117° 33' 44.20" W). This building was chosen for its unique architectural features, in which its walls are relatively flat with subtle texture. The amount of vegetation occluding the

building is minimal and despite its presence it can be filtered as shown in Figure 2.

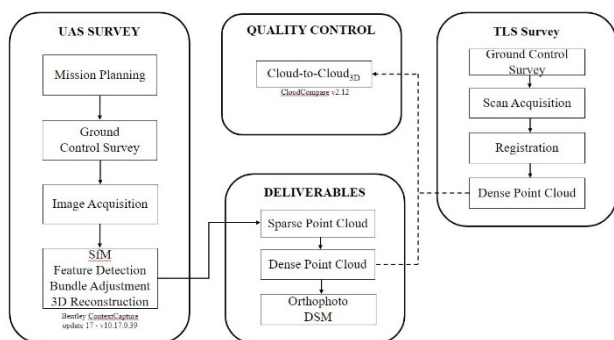


Figure 1. Flowchart of the Methodology.



Figure 2. Filtered building façade used for this study.

2.2 Image Acquisition

The images were acquired from a Phantom 4 Pro v2.0. The UAS was equipped with a 20 megapixels camera sensor (5,472 × 3,648) and a mechanical shutter. The shutter speed was adjusted based on lighting condition, UAS speed, and flight altitude at flight time to minimize image blurring. The mission was carried out autonomously using the software DroneDeploy, where a total of three different flights were performed. Flight 1, 2, and 3 had a flying height of 30, 46, and 46 meters, respectively. In addition, flight 3 was flown following an orbital path around the building at a flying altitude of 24 meters. The forward and side overlap for all flights was 80 and 70 %, respectively.

2.3 Ground Control Points

Prior to the image acquisition, six Ground Control Points (GCPs) were set around the project site to be used in the aerotriangulation. The three-dimensional coordinates of the GCPs were measured first with a Global Navigation Satellite System (GNSS) rover in Real-Time Kinematic (RTK) mode, with the base station located within the project site. Subsequently, the GCPs were measured with a total station for verification. The difference when comparing the traverse between the GNSS RTK and total station measurements was observed to have a total closure error of 0.012 meters and 00° 00' 02". The horizontal coordinates were processed to the California State Plane Coordinate System Zone 5, while the vertical was in the North American Vertical Datum of 1988. The base and rover

were Trimble R10 systems, while the total station was a Trimble S7.

2.4 Photogrammetric Processing

The photogrammetric process was carried out using Bentley ContextCapture, update 17 - v10.17.0.39. This photogrammetric software is based on the structure-from-motion methodology. The workflow follows a four-step process. The first step is to import the imagery and GCPs. The second step is to perform the photo ID to identify all GCPs/checkpoints in all corresponding images. The third step is to align the images by automatic feature identification and matching. The software simultaneously estimates both the internal and external parameters, including radial and tangential distortion. The result of this step is the camera position corresponding to each image, the internal camera calibration parameters, and the 3D coordinates of a sparse point cloud of the terrain. The final step is to create the dense point cloud and apply texture to the mesh. In general, the bundle adjustment can be carried out using a minimum of three GCPs; however, better results are obtained using more GCPs, which is recommended to achieve the best accuracy.

2.5 Terrestrial Laser Scanning

A Trimble TX8 laser scanner was used to capture the 3D point cloud of the building, which served as the ground truth for comparing the UAS point clouds from the three flights. This survey was performed by scanning the parking lot at six scan stations and georeferenced using spheres placed strategically to be visible from at minimum two scan stations. The spheres were placed by using a 2 m rod and bipod at each sphere station. Registration of the six Terrestrial Laser Scanning (TLS) point clouds was performed using Trimble RealWorks software. Upon completing the registration, a visual inspection was performed to ensure proper registration. Subsequently, the point clouds were segmented and filtered as shown in Figure 2. The final processing steps are similar to those from the UAS point clouds, which consist of the preparation of the point clouds to be imported into CloudCompare, where the TLS point cloud will be evaluated against the three UAS point clouds.

2.6 Cloud-to-Cloud Comparison

The point cloud analysis compared the UAS and TLS point clouds. It is important to note that performing a cloud-to-cloud (C2C) comparison is challenging due to the irregular point spacing from the UAS and TLS point cloud datasets, and no commonly recognized method currently exists for assessing point cloud accuracy (Mora et al., 2019) related to building façade reconstruction. For these reasons, we chose to perform a Cloud-to-Cloud (C2C) absolute distance comparison in CloudCompare by computing the nearest neighbor distance between the reference (i.e., ground truth/TLS point cloud) and the compared cloud (i.e., UAS point cloud). In this approach, the Euclidean distance is computed between each point in the compared cloud with the nearest point in the reference cloud (Mora et al., 2019). The analysis involved both a tabular summary and visualization to reveal spatial patterns between the two-point clouds. It is noted that only a portion of the north, south, east, and west wall was chosen to evaluate the spatial trends within the building. Each section evaluated (outlined in red in Figure 3) was selected due to their planar geometry. Flight 1, 2, and 3 will be referred to as Test 1, 2, and 3, respectively, herein.



Figure 3. Building façade areas to be compared between UAS and TLS point clouds are outlined in red for each wall.

3. RESULTS

The results are summarized in Table 1 and are shown as box plots in Figure 4 for all three tests along the north, south, east, and west walls. To evaluate the performance of each test, the overall mean, median, standard deviation, minimum, and maximum C2C distances are considered. The size of the area of interest, is expected to be a representative sample of the building façade planar geometry. Despite taking careful consideration to identify areas of interest along each wall, not every test produced clear results. This is apparent in the south wall for test 1 and 2 shown in Figure 5. A reason may be due to a “rip” in the scans present in tests 1 and 2, where there are excessive light levels (Gaulton and Malthus, 2010). The extreme light levels can also be seen in test 3 for the north and east walls and the laser scans of both the south and eastern walls. Another potential explanation is a combination of the area of interest and its proximity to windows, as it has been suggested to affect point cloud accuracy in previous studies (Mian et al., 2014; Koivumäki et al., 2021). For these reasons, the south wall area of interest for test 1 and test 2 are limited as shown in Table 1.

The box plots in Figure 4 comprise information related to the mean and standard deviations along all four walls for the three tests. Reviewing Table 1 and comparing the results with Figure 4, it appears that test 3 performs better overall compared to either test 1 or 2. This conclusion is apparent in the south and west walls, as test 3 has a significantly lower error than its counterparts. Unfortunately, in the north and south walls, test 2

appears to perform better. This can be attributed to the clarity of the scans that test 3 produces, as shown in Figure 3. In Figure 3, the north and south walls have some gaps, whereas these same walls in test 2 do not have gaps in the data. Since the primary change between each test is the flying height, the angles in which the UAS imagery is acquired from may produce some levels of light distortion that could have affected the point cloud (Mancini et al., 2013), especially for a light texture less wall. Another critical factor that could have affected the results is the time of day at which each flight was performed. Several previous studies have speculated that light levels and angle of reflections have adverse effects upon the cloud point accuracy (Ishida, 2017; Álvares et al., 2018). For this reason, it is suggested that future research also consider this factor when performing image acquisition from a UAS.

Test 1					
Wall	Mean (m)	Median (m)	STD (m)	Min (m)	Max (m)
North	0.016	0.013	0.013	0.000	0.061
South	0.514	0.535	0.264	0.000	1.014
East	0.050	0.043	0.040	0.000	0.212
West	0.027	0.021	0.022	0.000	0.094
Total	0.152	0.153	0.085	0.000	0.345
Test 2					
North	0.016	0.013	0.013	0.000	0.061
South	0.060	0.050	0.042	0.000	0.137
East	0.014	0.011	0.013	0.000	0.118
West	0.021	0.012	0.022	0.000	0.123
Total	0.028	0.021	0.022	0.000	0.110
Test 3					
North	0.028	0.017	0.026	0.000	0.100
South	0.024	0.015	0.021	0.000	0.086
East	0.033	0.020	0.039	0.000	0.220
West	0.007	0.005	0.006	0.000	0.046
Total	0.023	0.014	0.023	0.000	0.113

Table 1. Summary of C2C absolute distance for each test along each wall.

This study aims to provide further insight into flying height and point cloud accuracy for building façade reconstruction. Using a TLS as a baseline, it is possible to determine the level of accuracy that can be obtained compared to a pre-established method that has historically shown high accuracy levels (Hackenberg et al., 2014; Li et al., 2020). In addition, this study aims to determine the optimal flying height that will lead to results with higher levels of accuracy and consistency. Test 3 provided a mean, median, and standard deviation of 0.023, 0.014, and 0.023 meters, respectively, outperforming both tests 1 and test 2. With these results, it is suggested that the UAS image acquisition with a flying height of 46 meters and an orbit of 24 meters produces favorable results and should be looked into further when conducting C2C analysis.

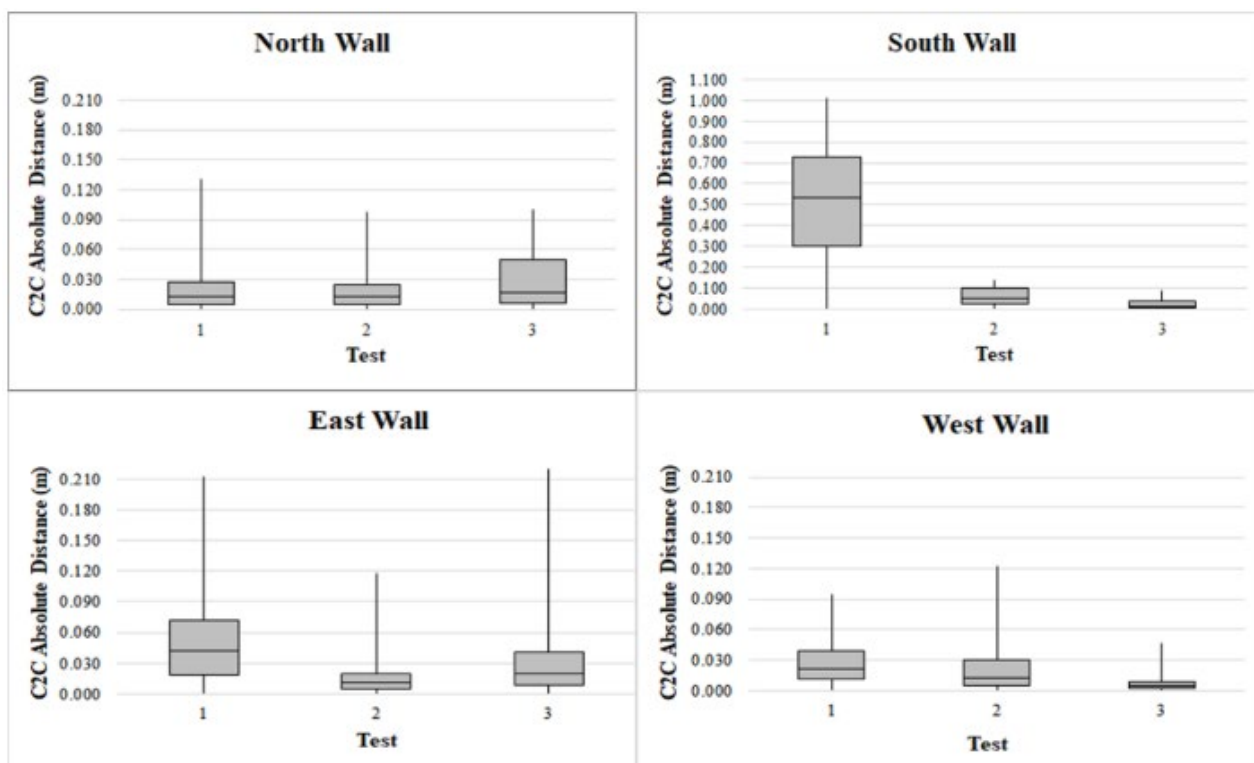


Figure 4. Box plots of C2C absolute distance for each test along each wall.

4. CONCLUSIONS

As a result of this study, the need for a more comprehensive study regarding the UAS flying height in which image acquisition is performed for building façade reconstruction is needed. The test that provided the best results in terms of C2C absolute distance is test 3, in which the UAS was flown at the height of 46 meters and an orbit of 24 meters. As this height changes, the quality of each UAS point cloud will vary; however, other factors outside of flying height will also influence the accuracy of the point clouds. The time of day is likely to affect the quality of each point cloud with the subsequent angle of the sun. The light levels are also a potential factor in the quality of UAS point clouds, which may or may not be amplified by the flying height of the UAS. For these reasons, this study considers these variables when evaluating the performance of building façade reconstruction from UAS imagery.

In this study, the best results were obtained by determining which test yielded the lowest C2C absolute distance. Our results showed that test 3 yielded the lowest overall error with a mean, median, and standard deviation of 0.023, 0.014, and 0.023 meters, respectively, meeting sub-decimeter accuracy. Based on these results, UAS façade reconstruction is not only possible but can be preferred if traditional methods are not feasible as long as proper planning, data collection, and processing procedures are followed.

ACKNOWLEDGEMENTS

The authors want to thank the WestLAND Group, Inc. for helping with the data collection for this study.

REFERENCES

Aber, J. S., Marzloff, I., & Ries, J. (2010). Small-format aerial photography: Principles, techniques and geoscience applications. Elsevier.

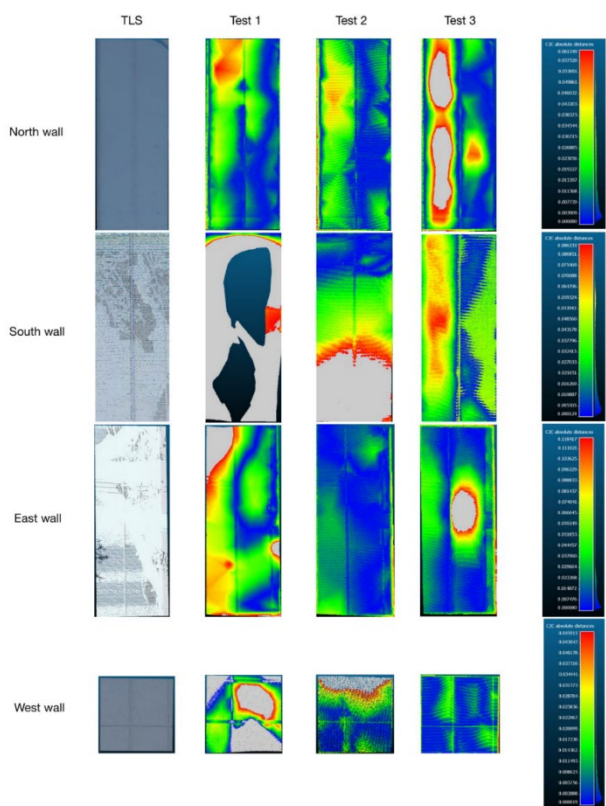


Figure 5. C2C results for test 1, 2, and 3 along the north, south, east, and west walls.

- Adams, S. M., Levitan, M. L., & Friedland, C. J. (2014). High resolution imagery collection for post-disaster studies utilizing unmanned aircraft systems (UAS). *Photogrammetric Engineering & Remote Sensing*, 80(12), 1161-1168.
- Ajayi, O. G., Palmer, M., & Salubi, A. A. (2018). Modelling farmland topography for suitable site selection of dam construction using unmanned aerial vehicle (UAV) photogrammetry. *Remote Sensing Applications: Society and Environment*, 11, 220-230.
- Álvares, J. S., Costa, D. B., & de Melo, R. R. S. (2018). Exploratory study of using unmanned aerial system imagery for construction site 3D mapping. *Construction Innovation*.
- Colomina, I., & Molina, P. (2014). Unmanned aerial systems for photogrammetry and remote sensing: A review. *ISPRS Journal of photogrammetry and remote sensing*, 92, 79-97.
- Díaz-Vilariño, L., González-Jorge, H., Martínez-Sánchez, J., Bueno, M., & Arias, P. (2016). Determining the limits of unmanned aerial photogrammetry for the evaluation of road runoff. *Measurement*, 85, 132-141.
- Erlanson, J. P., & Veress, S. A. (1974). Contemporary problems in terrestrial photogrammetry. *Photogrammetric Engineering*, 40(9), 1079-1085.
- Eschmann, C., Kuo, C. M., Kuo, C. H., & Boller, C. (2012). Unmanned aircraft systems for remote building inspection and monitoring.
- Gabrlík, P. (2015). The use of direct georeferencing in aerial photogrammetry with micro UAV. *IFAC-PapersOnLine*, 48(4), 380-385.
- Galantucci, R. A., & Fatiguso, F. (2019). Advanced damage detection techniques in historical buildings using digital photogrammetry and 3D surface analysis. *Journal of Cultural Heritage*, 36, 51-62.
- Gaulton, R., & Malthus, T. J. (2010). LiDAR mapping of canopy gaps in continuous cover forests: A comparison of canopy height model and point cloud based techniques. *International Journal of Remote Sensing*, 31(5), 1193-1211.
- Grussenmeyer, P., Landes, T., Voegtle, T., & Ringle, K. (2008). Comparison methods of terrestrial laser scanning, photogrammetry and tacheometry data for recording of cultural heritage buildings. *International Archives of Photogrammetry, Remote Sensing and Spatial Information Sciences*, 37(B5), 213-218.
- Hackenberg, J., Morhart, C., Sheppard, J., Spiecker, H., & Disney, M. (2014). Highly accurate tree models derived from terrestrial laser scan data: A method description. *Forests*, 5(5), 1069-1105.
- Ishida, K. (2017). Investigating the accuracy of 3D models created using SfM. In *ISARC. Proceedings of the International Symposium on Automation and Robotics in Construction (Vol. 34)*. IAARC Publications.
- Kim, M., Park, S., Irwin, J., McCormick, C., Danielson, J., Stensaas, G., ... & Burgess, M. (2020). Positional Accuracy Assessment of Lidar Point Cloud from NAIP/3DEP Pilot Project. *Remote Sensing*, 12(12), 1974.
- Koivumäki, P., Steinböck, G., & Haneda, K. (2021). Impacts of point cloud modeling on the accuracy of ray-based multipath propagation simulations. *IEEE Transactions on Antennas and Propagation*.
- Li, Y., Su, Y., Zhao, X., Yang, M., Hu, T., Zhang, J., ... & Guo, Q. (2020). Retrieval of tree branch architecture attributes from terrestrial laser scan data using a laplacian algorithm. *Agricultural and Forest Meteorology*, 284, 107874.
- Mancini, F., Dubbini, M., Gattelli, M., Stecchi, F., Fabbri, S., & Gabbianelli, G. (2013). Using unmanned aerial vehicles (UAV) for high-resolution reconstruction of topography: The structure from motion approach on coastal environments. *Remote sensing*, 5(12), 6880-6898.
- Martinez, J. G., Albeaino, G., Gheisari, M., Volkmann, W., & Alarcón, L. F. (2021). UAS Point Cloud Accuracy Assessment Using Structure from Motion-Based Photogrammetry and PPK Georeferencing Technique for Building Surveying Applications. *Journal of Computing in Civil Engineering*, 35(1), 05020004.
- Mian, S. H., Mannan, M. A., & Al-Ahmari, A. M. (2014). The influence of surface topology on the quality of the point cloud data acquired with laser line scanning probe. *Sensor Review*.
- Mikhail, E. M., Bethel, J. S., & McGlone, J. C. (2001). *Introduction to modern photogrammetry*. New York, 19.
- Mora, O.E., Suleiman, A., Chen, J., Pluta, D., Okubo, M.H. and Josenhans, R., 2019. Comparing sUAS Photogrammetrically-Derived Point Clouds with GNSS Measurements and Terrestrial Laser Scanning for Topographic Mapping. *Drones*, 3(3), p.64.
- Peppas, M. V., Hall, J., Goodyear, J., & Mills, J. P. (2019). PHOTGRAMMETRIC ASSESSMENT AND COMPARISON OF DJI PHANTOM 4 PRO AND PHANTOM 4 RTK SMALL UNMANNED AIRCRAFT SYSTEMS. *International Archives of the Photogrammetry, Remote Sensing & Spatial Information Sciences*.
- Rakha, T., & Gorodetsky, A. (2018). Review of Unmanned Aerial System (UAS) applications in the built environment: Towards automated building inspection procedures using drones. *Automation in Construction*, 93, 252-264.
- Shashi, M., & Jain, K. (2007). Use of photogrammetry in 3D modeling and visualization of buildings. *ARPJ Journal of Engineering and Applied Sciences*, 2(2), 37-40.
- Sowmya, A., & Trinder, J. (2000). Modelling and representation issues in automated feature extraction from aerial and satellite images. *ISPRS journal of photogrammetry and remote sensing*, 55(1), 34-47.
- Whitehead, K., Moorman, B. J., & Hugenholtz, C. H. (2013). Brief Communication: Low-cost, on-demand aerial photogrammetry for glaciological measurement. *The Cryosphere*, 7(6), 1879-1884.